PHYSICAL REVIEW B VOLUME 53, NUMBER 19 15 MAY 1996-I

Interlayer interactions in LiC_6: Compressibility and thermal expansion

Ping Zhou and John E. Fischer
Department of Materials Science and Engineering, University of Pennsylvania, Philadelphia, Pennsylvania 19104-6272
and Laboratory for Research on the Structure of Matter, University of Pennsylvania, Philadelphia, Pennsylvania 19104-6272

(Received 11 December 1995)

Interlayer interactions in the prototype stage-1 graphite intercalation compound LiC_6 are probed by neutron diffraction measurements of c-axis compressibility κ_c at 300 K and c-axis thermal expansion α_c in the interval 300–700 K. We find a constant $\kappa_c = 1.43 \pm 0.02 \times 10^{-12}$ cm^2/dyn for hydrostatic pressures $\leqslant$ 23 kbar, about half that of graphite. In contrast, $\alpha_c = 59 \times 10^{-6}$/K, twice that of graphite. Estimates of effective c-axis Grüneisen parameters show that the interlayer potential in LiC_6 is in fact considerably more anharmonic than that of graphite. Measurements of α_c on high temperature stage-1 solid solutions suggest even greater anharmonicity when 30% of the Li sites are vacant. [S0163-1829(96)02020-6]

Graphite is the prototype layer solid. The interlayer van der Waals bonding is well represented by a Lennard-Jones potential,[1] from which one expects, and observes, important anharmonic effects associated with the steep repulsive r^{-12} term: large c-axis thermal expansion, departures from Hooke's law at modest c-axis compressions, etc. Intercalation with alkali metals introduces new contributions, namely, the electrostatic interaction between oppositely charged carbon and metal layers and carbon-metal core repulsion, and also modifies the van der Waals contribution by dilating the lattice. The net effect is an increase in interlayer force constants, c-axis sound velocities, longitudinal $(00L)$ phonon energies etc.,[2] i.e., a general stiffening of the potential. On the other hand, little is known about the effect of intercalation on its shape, that is, the extent to which anharmonic properties are altered.

LiC_6 is one of the most thoroughly studied alkali-graphite compounds,[3,4] and it plays an important role in understanding the performance of carbon-based anodes in rechargeable Li-ion batteries.[5] Upon intercalation, some fraction of the Li $2s$ valence electron density becomes delocalized on the carbon layers, and the intralayer Coulomb repulsion between Li ''ions'' competes with the attractive interaction between oppositely charged Li and C layers, the former becoming the density-limiting factor. The Li ''cations'' form a commensurate $\sqrt{3}a \times \sqrt{3}a$ superlattice in the gallery where $a=$ 2.46 Å is the graphite in-plane lattice constant. The c-axis stacking sequence is $A\alpha A\alpha, \ldots,$ where A and α represent carbon and Li layers, respectively. Thus all the interlayer C-C and Li-Li neighbor pairs are eclipsed, in contrast to the situation in graphite ($ABAB$ stacking) in which only half the C-C pairs are eclipsed, the other half being staggered.

The elastic and thermal properties of graphite have been extensively studied experimentally (e.g., x-ray[6–8] and inelastic neutron scattering[9]) and very well understood theoretically.[1] Results on the intercalation compounds are more limited. Phonon spectra have been exploited to estimate adiabatic elastic constants, in particular C_{33} from the low-Q slope $d\omega/dQ$ of longitudinal $(00L)$ modes. Values for LiC_6 vary considerably: 8.9,[10] 7.1,[11] and 5.8,[12] all in units of $10^{11}\mathrm{dyn/cm}^2$. A Thomas-Fermi density-functional calculation[13] predicted the correct trend of elastic constants for different alkali metals but the absolute values were not well reproduced, the predicted C_{33} for LiC_6 being nearly twice the largest phonon-derived value.

Here we address the anharmonicity of the interlayer potential in LiC_6 by measuring the isothermal c-axis compressibility and thermal expansion using neutron diffraction. LiC_6 was prepared from highly oriented pyrolytic graphite by immersion in molten Li at 250 °C.[14] Compressibility was determined from the variation in c with hydrostatic pressure, using a cell described in the literature.[15] Pieces of LiC_6 and undoped HOPG were cut to fit loosely in a lead-plated Al capsule 6 mm in diameter and 14 mm long (the latter serving as a pressure gauge), the remaining volume being filled with Fluorinert FC-75, which remains fluid up to 50 kbar at 300 K and does not react with Li or LiC_6. Pressure was applied with a hydraulic press. Samples for thermal expansion were enclosed in welded stainless steel foil envelopes in an Ar-filled glove box and measured in a convectively heated furnace with temperature control and measurement by two separate thermocouples. Both experiments were carried out on the H4S triple-axis neutron spectrometer at the Brookhaven High Flux Beam Reactor, using typical collimation of 20′-20′-20′-20′, graphite (002) monochromator ($\lambda = 2.37$ Å) and (004) analyzer yielding typical longitudinal resolution of 0.01 Å^{-1}. Lattice constants versus T or P were derived from Gaussian fits to two reflections [graphite (002) and (004), LiC_6 (001), and (002)] to account for zero error in diffraction angle. Counting statistics were large enough to ensure standard deviations in fitted positions of no greater than ± 0.003 Å. A typical example is shown in the inset to Fig. 1.

Pressure versus hydraulic load was determined from the measured graphite c parameter and an empirical relation from pressure-dependent x-ray diffraction:[6]

$$c/c_0 = [(\zeta'/\zeta_0)P + 1]^{-1/\zeta'}, \tag{1}$$

where c_0 is the lattice constant at zero pressure (3.357 Å), ζ (= 360 kbar), and ζ' (= 10) are the c-axis compliance (i.e., the inverse of the c-axis compressibility) and its dimensionless pressure derivative, respectively. We note in passing

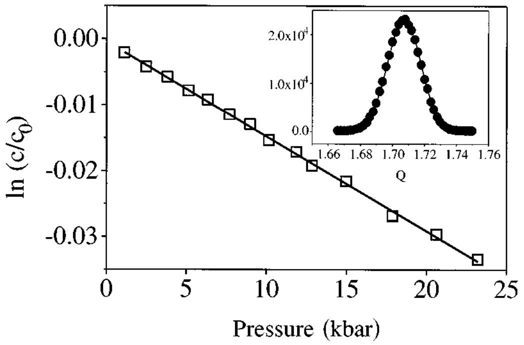

FIG. 1. Pressure dependence of the (normalized) LiC_6 c-axis lattice constant from $(00L)$ neutron diffraction (squares). Extrapolated $c_0 = 3.701$ Å. The solid line is a linear fit. Inset: typical (001) profile (dots) and a Gaussian fit (solid curve) at 3.81 kbar.

that ζ for highly oriented pyrolitic graphite (HOPG) agrees with a linear compliance based on $(00L)$ phonons,[9] namely, $3.58 \pm 0.1 \times 10^{11}$ dyn/cm^2. The nonlinearity in graphite becomes significant when $c/c_0 \leqslant 0.97$, well below our maximum pressure. This is observed in a raw plot of LiC_6 versus graphite peak positions (not shown) as a distinct positive curvature, suggesting at first glance that graphite is more anharmonic than LiC_6 since its ζ' must be the more positive. This turns out to be misleading, as discussed later.

The normalized lattice constant c/c_0 of LiC_6 is plotted as a function of pressure in Fig. 1. A maximum contraction of 3% is achieved at our pressure limit of 23 kbar, set by the collapse of the Al cell to the point at which it crushes the sample and degrades the c-axis mosaic. As noted above, graphite has already become noticeably nonlinear at this degree of contraction, whereas the LiC_6 data in Fig. 1 are very well fit by a constant compressibility, $\kappa_c = 1.43 \pm 0.02 \times 10^{-12}$ cm^2/dyn. Since C_{13} in LiC_6 is essentially zero due to the eclipsed stacking,[7] to a good approximation $C_{33} = 1/\kappa_c = 6.97 \pm 0.09 \times 10^{11}$ dyn/cm^2, 90% larger than that of graphite. An upper bound on the pressure dependence of κ_c was obtained by fitting the same data to a polynomial:

$$\ln(c/c_0) = \kappa_0 - \kappa_c' P - \kappa_c' P^2/2, \qquad (2)$$

where κ_c' represents the pressure derivative. From the standard deviation we estimate $\kappa_c' \leqslant 5.4 \times 10^{-15}$ cm^2/dyn/kbar, or in terms of Eq. (1), $\zeta' \leqslant 2.6$, much less than the value 10 for graphite. We conclude that the interlayer potential in LiC_6 remains quite parabolic up to a 3% reduction in interlayer spacing.

The thermal variation of c for LiC_6 is shown in Fig. 2, along with a linear fit which gives an average α_c over the range 320–680 K of 59×10^{-6}/K, more than a factor of 2 larger than that of graphite (27×10^{-6}/K at comparable temperatures[8]). Taken at face value, this suggests that LiC_6 is more anharmonic than graphite. Also plotted in Fig. 2 are data for $\mathrm{Li}_x\mathrm{C}_6$ ($x = 0.89$ and 0.69).[12] These are two-phase mixtures of stage-1 LiC_6 and stage-2 LiC_{12} at low temperature, transforming to single-phase "dilute stage 1" at high temperature. This provides a convenient approach for studying the dependence of various properties on in-plane density.[4] Just below the transition the c parameter actually contracts with increasing T, a consequence of Li leaving the fully occupied stage-1 galleries (and entering the empty galleries in stage 2). Linear behavior is recovered above the transition, giving $\alpha_c = 76$ and 110×10^{-6}/K for stage 1 with 11% and 31% vacant Li sites, respectively, i.e., even more strongly anharmonic behavior with decreasing Li density.

Anharmonicity in structural energies is quantified by the Grüneisen parameter, a direct measure of the nonparabolic potential:

$$\gamma \equiv -\sum_i \int e_i(q) \frac{\partial \ln \omega_i(q)}{\partial \ln V} dq \Bigg/ \sum_i \int e_i(q) dq, \qquad (3)$$

where $\omega_i(q)$ is the ith phonon frequency, $e_i(q)$ is the Einstein specific-heat function, q is the phonon wave vector, and

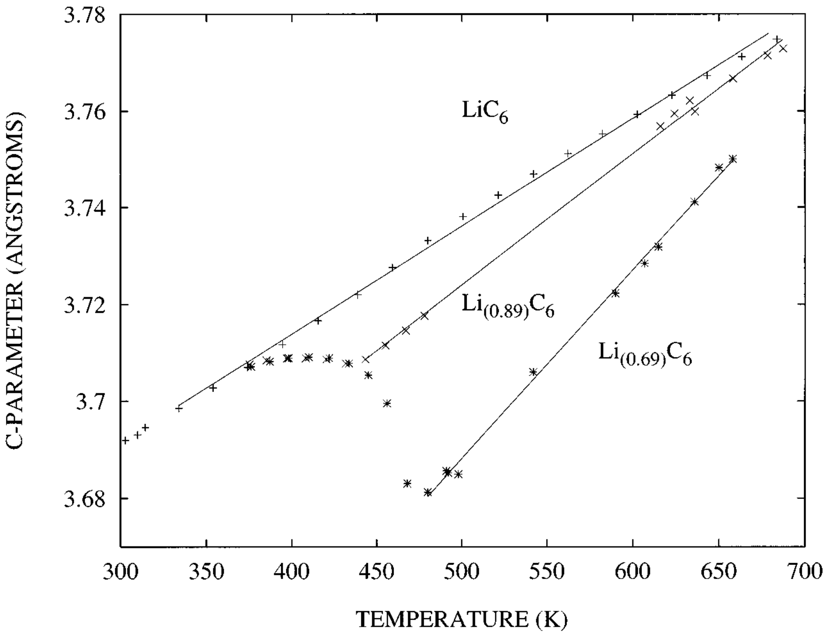

FIG. 2. Temperature dependence of c for pure stage-1 $\mathrm{Li}_x\mathrm{C}_6$ with $x = 1(+)$, $0.89(\times)$, and $0.69(*)$. Solid lines are linear fits, which for the latter two are restricted to temperatures above the phase transitions ending at 450 and 500 K, respectively. Note the strong increase in dc/dT with increasing Li vacancy concentration.

TABLE I. Comparison of c-axis elastic parameters, thermal expansion coefficients, and interlayer Grüneisen parameters for graphite and stage-1 intercalation compounds. C_{33} values for graphite derived from LA phonons and diffraction vs pressure are in good agreement (see text); the entries for MC_8 are based on LA phonon dispersion. The last column is the inverse of the intercalate mass per unit area.

	C_{33} 10^{11} dyne/cm^2	α_c 10^{-6}/K	γ_c	1/areal mass 10^{23} g^{-1}
Graphite	3.7 [9]	24±4 [17]	0.58±0.09	-
CsC_8	5.83±0.12 [2]	28±6 [17]	0.9±0.2	0.36
RbC_8	4.84 [2]	30±7 [17]	0.80±0.2	0.56
KC_8	4.85±0.14 [2]	45±8 [17]	1.2±0.2	1.20
LiC_6	6.97±0.09 (this work)	59 (this work)	1.80±0.02 (this work)	5.13
$Li_{0.89}C_6$	-	76 [12]	-	5.76
$Li_{0.69}C_6$	-	110 [12]	-	7.43

V is the volume. In the simplest cases $\gamma = \alpha_V V/\kappa_T C_V$ where α_V is the volume thermal expansion and κ_T the isothermal compressibility. For parabolic potentials the ω's are V independent, $\alpha_V = 0$ and hence $\gamma = 0$. Girifalco has pointed out the need for caution when applying the simple form to solids with distinctly different kinds of bonds, viz., the strong intraball versus weak interball bonds in solid C_{60}.[16] Similarly, we require an effective interlayer Grüneisen parameter γ_c for layer compounds, involving the contribution to C_V from the interlayer modes alone, which we estimate from the thermal energy of the longitudinal phonons:[17]

$$E_{\text{therm}}(T) = \frac{c_0}{\pi}\int \frac{dq}{d\omega}\,\frac{\hbar\omega}{e^{\hbar\omega/k_BT}-1}\,d\omega, \tag{4}$$

where $dq/d\omega$ is obtained from $(00L)$ phonon dispersion fitted to a shell model using force constants from Ref. 2. We emphasize that γ_c as defined herein is useful only for comparing the anharmonicities of interlayer potentials in two-dimensional systems; in particular, γ_c's cannot be compared with the isotropic γ's of cubic systems.

For LiC_6 the temperature derivative of E_{therm} gives a heat capacity 0.138 meV/K at 300 K for a cell volume $V = \sqrt{3}/4a^2c$, where a and c are 2.46 and 3.70 Å, respectively. Combined with the measured α_c and κ_c, we find $\gamma_c = 1.80$ for LiC_6, more than a factor of 3 larger than that of graphite (0.58) obtained in the same way. In Table I we collect C_{33}, α_c, and γ_c values for graphite, LiC_6, and MC_8 compounds (M = Cs, Rb, and K) (Refs. 2 and 17) along with α_c for Li_xC_6 with $x = 0.89$ and 0.69. The inverse of the intercalate areal mass is also included in Table I. The stiffness constant C_{33} is the second derivative of the interlayer potential on the repulsive side and carries limited information regarding the overall shape of the potential. Thus it does not exhibit any systematic behavior for the different materials. On the other hand, α_c is larger in the compounds than in graphite, indicating more anharmonic potentials in the former. It increases as the intercalant mass decreases, due to larger amplitude thermal motions of lighter cations at the same temperature. The exceptionally large α_c in Li_xC_6 ($x = 0.89$ and 0.69) follows the same trend, the Li's being effectively ''lighter'' as they become decoupled due to the vacant sites.

Within error bars, the overall anharmonicity reflected by γ_c scales linearly with the inverse of the intercalate areal mass, consistent with the notion that the lightest ''layers'' undergo the most violent thermal excursions and hence sample the nonparabolic part of the potential to the largest extent. As noted above and elsewhere,[17] material variations in γ_c are dominated by variations in α_c; in particular, application of Eq. (4) shows that the thermal energies for the dilute stage-1 solid solutions are not very different from that of LiC_6, the main effect of Li vacancies being an increase in the energy of the optical branch while E_{therm} is dominated by the acoustic modes in this range of temperature. Thus we expect γ_c for the dilute solid solutions to be even larger than for LiC_6. C_{33} data would be required to prove this, for example, by measuring $(00L)$ phonons at high temperature on samples with $x<1$. It would also be of interest to explore the thermal and elastic properties for $x>1$, i.e., the high-pressure phase LiC_2.[18]

Table II gives a summary of the various determinations of C_{33} for LiC_6. As noted above, values derived from long-wavelength phonon dispersion are adiabatic and are related to the isothermal value according to $\kappa_T/\kappa_S = C_P/C_V = 1 + \gamma\alpha T$ where C_P and C_V are the constant pressure and constant volume heat capacities, respectively. Using the γ_c and α_c values from Table I, the adiabaticC_{33} deduced from LA phonons should be 3.2% greater than the diffraction-based value obtained from Fig. 1. The C_{33} determined by Rossat-Mignod *et al.*[11] agrees with our prediction well. The significant discrepancies among other numbers in Table II remain unexplained.

It has been shown from a numerical calculation based on the band structure that the electron density in LiC_6 is highly

TABLE II. C_{33} of LiC_6 obtained from diffraction and phonon measurements.

C_{33} 10^{11} dyne/cm^2	Method
6.97±0.09	Diffraction (this work)
8.9	LA phonon [2]
7.1	LA phonon [11]
5.8	LA phonon [12]

nonhomogeneous and anisotropic.[19] ^{13}C NMR measurements revealed a Knight shift corresponding to an effective $0.74e^-$ charge transfer from Li to graphite[20] and a recent simulation also predicted a value of $0.6e^-$.[21] Therefore, the concept of complete ionization is not very accurate in this particular system. This could be the main reason that the Thomas-Fermi density-functional calculation (based on the assumption of complete charge transfer) (Ref. 13) predicted a C_{33} twice as large as the experimental result. Further calculation of the total energy of LiC_6 based on the electron density in Ref. 19 is in progress.

We thank L. A. Girifalco and E. J. Mele for helpful discussions, and P. Wochner and D. B. McWhan for assistance with the pressure cell. This work was supported by the Hughes Aircraft Co. and by the Department of Energy, DEFC02-86ER45254. The Brookhaven HFBR is supported by DOE, Division of Materials Sciences, DEAC02-76CH00016.

---

[1] L. A. Girifalco and R. A. Lad, J. Chem. Phys. **25**, 693 (1956).

[2] H. Zabel, in *Graphite Intercalation Compounds I: Structure and Dynamics*, edited by H. Zabel and S. A. Solin (Springer, New York, 1990), p. 101.

[3] D. Guerard and A. Herold, Carbon **13**, 337 (1975).

[4] J. E. Fischer, in *Chemical Physics of Intercalation*, edited by A. P. Legrand and S. Flandrois (Plenum, New York, 1987), p. 59.

[5] J. R. Dahn, T. Zheng, Y. Liu, and J. S. Xue, Science **270**, 590 (1995).

[6] M. Hanfland, H. Beister, and K. Syassen, Phys. Rev. B **39**, 12 598 (1989).

[7] Y. X. Zhao and I. L. Spain, Phys. Rev. B **40**, 993 (1989).

[8] J. B. Nelson and D. P. Riley, Proc. Phys. Soc. A **57**, 160 (1945).

[9] R. Nicklow, N. Wakabayashi, and H. G. Smith, Phys. Rev. B **5**, 4951 (1972).

[10] H. Zabel, A. Magerl, and J. J. Rush, Phys. Rev. B **27**, 3930 (1983).

[11] J. Rossat-Mignod *et al.*, Synth. Met. **2**, 143 (1980).

[12] J. E. Fischer (unpublished).

[13] D. P. DiVincenzo and E. J. Mele, Phys. Rev. Lett. **53**, 52 (1984).

[14] M. Zanini, S. Basu, and J. E. Fischer, Carbon **16**, 211 (1978).

[15] D. B. McWhan, C. Vettier, R. Youngblood, and G. Shirane, Phys. Rev. B **20**, 4612 (1979).

[16] L. A. Girifalco, Phys. Rev. B **52**, 9910 (1995).

[17] S. E. Hardcastle and H. Zabel, Phys. Rev. B **27**, 6363 (1983).

[18] V. V. Avdeev, V. A. Nalimova, and K. N. Semenenko, High Press. Res. **6**, 11 (1990); V. A. Nalimova, D. Guerard, M. Lelaurain, and O. V. Fateev, Carbon **33**, 177 (1995).

[19] L. A. Girifalco and N. A. W. Holzwarth, Mat. Sci. Eng. **31**, 201 (1977).

[20] J. Conard *et al.*, Physica B **99**, 521 (1980).

[21] P. Pananek, M. Radosavljevic, and J. E. Fischer, Chem. Mater. (to be published).